Appl. Phys. A 76, 1013–1016 (2003)
DOI: 10.1007/s00339-002-1942-2

Applied Physics A
Materials Science & Processing

K. WANG[1,✉]
A. CHELNOKOV[2]
S. ROWSON[2]
J.-M. LOURTIOZ[2]

Extremely high-aspect-ratio patterns in macroporous substrate by focused-ion-beam etching: the realization of three-dimensional lattices

[1] Laboratoire de Physique des Solides, CNRS (UMR8502), Bât. 510, 91405 Orsay, France
[2] Institut d'Électronique Fondamental, CNRS (UMR8622), Bât. 220, 91405 Orsay, France

Received: 21 August 2002 /Accepted: 21 August 2002
Published online: 12 February 2003 •

ABSTRACT We show the very particular behavior of focused-ion-beam etching in macroporous silicon. We demonstrate that, contrary to bulk samples, a porous substrate allows extremely high-aspect-ratio patterns to be etched at submicrometer scales. Thanks to the pre-introduced porosity, the secondary effects that limit the pattern depth in bulk-sample etching, namely the sputtered material redeposition as well as the beam 'self-focusing' effects, are strongly reduced in a porous sample. In this case the walls between the pores are sputtered in an almost independent way. The etching of deep and straight patterns is feasible. Combined with photoelectrochemical etching that generates the initial macropores, three-dimensional (3D) lattices can be obtained, as demonstrated by 3D photonic crystal fabrication.

PACS 85.40.Hp; 81.05.Rm

1 Introduction

The focused-ion beam (FIB) is widely employed for mask-less dry etching that is much more flexible than traditional etching methods [1]. It can be used in particular to etch patterns at any angle with respect to the substrate surface. This allows us to obtain structures defined by more than one axis and thus provides the possibility to etch three-dimensional (3D) lattice structures.

This is, however, difficult to achieve in practice due to a major drawback of the FIB etching: it is impossible to produce deep patterns in a bulk substrate, where, limited by several secondary effects intrinsic to FIB etching [2, 3], the aspect ratio (width/depth) remains too weak for 3D lattices.

In this work we will show that if, instead of bulk substrates, the FIB etching is performed on a porous one, the etching of extremely deep high-aspect-ratio holes becomes feasible even at the submicrometer scale. 3D lattice structures can thus be achieved. We will apply this method to the fabrication of 3D photonic crystals in the near-infrared range, which, due to the short wavelength, are characterized by periods of submicrometer scale.

✉ Fax: +33-1/6915-6086, E-mail: wang@lps.u-psud.fr

2 FIB etching of porous substrate

It is observed that, when etching bulk substrates using a FIB, the etched depth varies non-linearly with the etching time. During the etching, the sputter rate first increases and then decreases down to almost zero, thus limiting the depth of the pattern. The sputter-rate saturation can be clearly observed at less than 2-μm depth for a trench width below 1 μm [3]. Moreover, the resulting trench has a V-shaped profile [2, 3]. An aspect ratio not greater than eight has been observed when etching bulk silicon with a 30-keV Ga^+ beam [2].

The origins of these phenomena are attributed to the Gaussian profile of the ion beam and to several secondary effects related to the beam–substrate interaction, mainly the ion-beam reflection by the side walls of the trench ('self-focusing') that modifies the beam profile by concentrating the incident ions to the center of the trench, as well as the redeposition of the sputtered material that tends to 'refill' the trench [2, 3]. Chemically assisted etching allows a greater sputter rate, but only a slight aspect-ratio increase is observed (10 instead of eight) [4].

A 3D lattice needs deep and straight holes to be drilled in the substrate. Therefore, the above limiting effects must be eliminated, or, at least, sufficiently reduced. Independently of the etched material, the amplitude of the Gaussian wings in the FIB profile can be diminished by using a weak emission current in order to limit the ion-energy spread [5]. The substrate-related-effect elimination will imply substrate modifications. In this perspective, porous substrates can be used instead of bulk ones. This choice is motivated by the following considerations.

On one hand, in a porous substrate, the material to sputter is the walls between the pores. There is much less material to evacuate, depending on the substrate air-filling rate. The higher the latter, the less the sputtered material. Further, the presence of the pores facilitates the evacuation of the sputtered material, most of which will be projected into the pores rather than out of the substrate. The FIB will always meet pores whatever the etching depth is, so the material evacuation is always possible. Moreover, since the sputtered material is projected into the pores which are

separated by the walls, there is little correlation of material redeposition between the pores over the whole depth. The etching condition will remain almost identical for all the walls. Therefore the etching of very deep holes can be achieved.

On the other hand, for each hole to etch, the ion beam meets a series of walls, separated by pores. The side walls of the holes are thus discontinuous. Such a particular structure will strongly reduce the ion reflection by the side walls of the FIB-etched holes responsible for the self-focusing effect. Since these side walls are not continuous, it is difficult for incident ions to be 'bounced' continuously by the side walls and concentrated to the center of the holes. The ion current density profile will thus remain more uniform, and the hole side walls more straight.

In order to check the validity of the substrate choice, several porous samples are prepared and etched by a Ga^+ beam. The Ga^+ FIB is generated by a Canion ion gun, provided by Orsay Physics. It is connected to a home-built ultra-high-vacuum chamber. The residual pressure is maintained below 5×10^{-7} Pa. The sample holder is carried by a vibration-isolated UHV-compatible displacement table. The ion gun uses a hairpin-type needle to form the liquid-metal ion source. The ion beam is accelerated at the energy of 25 keV. The extraction voltage is adjusted so that a weak emission current, about 1 μA, is stabilized. This allows us to limit the ion-energy spread and thus the Gaussian wings in the FIB profile [5]. The beam is focused to a final spot of about 100 nm in size, with a spot current of about 30 pA. This current allows a reasonable etching rate at which the ion beam remains stable during the etching process.

The apparatus is equipped with an electron detector composed of a scintillator and a photomultiplier, allowing us to image the sample surface through secondary-electron collection. The etching process can also be monitored by secondary electron current measurements.

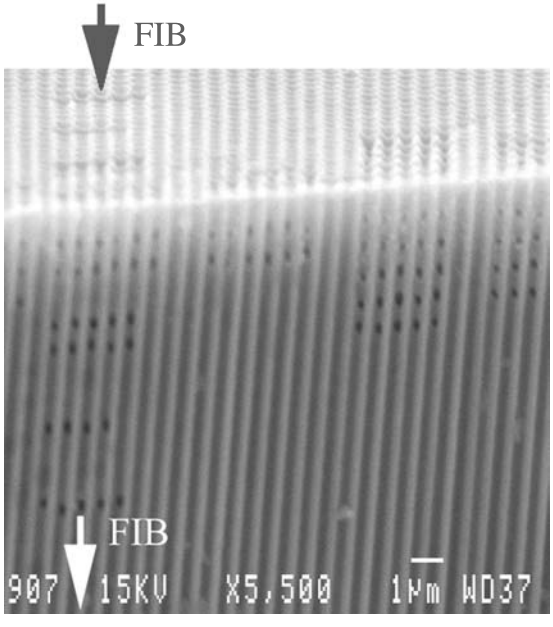

FIGURE 1 The scanning microscopy image of a macroporous substrate after FIB etching. The ion beam traverses the substrate and exits by its side

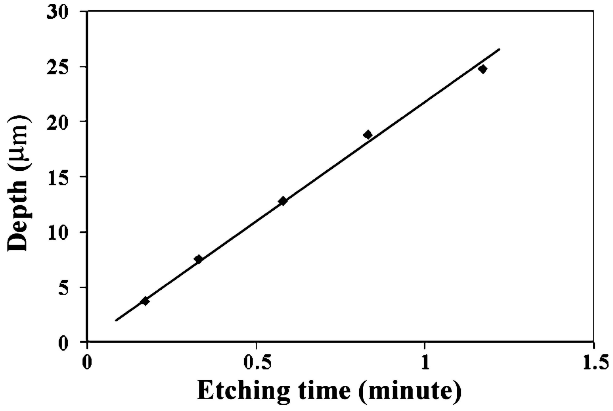

FIGURE 2 The FIB etching depth as a function of the etching time

The scanning electron microscopy image of a porous sample after FIB etching is displayed in Fig. 1. The sample has a so-called 'macroporous' structure. The porosity is introduced into the crystalline silicon substrate by photoelectrochemical etching [6]. The macropores (submicrometer holes) are perpendicular to the sample surface where their openings can be seen. The air-filling rate of the sample is about 40%. The FIB hits the sample at a glancing angle of about 30 degrees to the surface. It traverses the substrate and exits by its side.

Several series of holes are drilled through the sample. For each hole the etching is stopped when the beam traverses the sample and hits the sample holder, provoking a jump in the secondary-electron emission. This allows us to monitor the etching time for different hole lengths.

The holes have a diameter of about 0.3 μm. The deepest among them have a length of about 20 μm. The corresponding aspect ratio reaches 60, almost an order of magnitude higher than in the bulk substrate.

The etching speed is obtained by measuring the etching time of holes of various depths through secondary electron emission monitoring. A typical curve is plotted in Fig. 2 in an etching depth vs. time diagram. The etching speed remains constant to a depth of 25 μm. Neither initial speed increase, characteristic of the self-focusing effect in bulk substrates [3], nor final speed saturation, that occurs at a depth of less than 2 μm for a submicrometer trench width in bulk substrates [3], are observed. This shows clearly that the substrate-related secondary effects are effectively eliminated in a porous sample.

The above results demonstrate the particular behavior of the FIB in a porous substrate. Moreover, it is worth noting that in the case of bulk substrates quoted above [2, 3] the etched patterns are trenches, while in the present case they are holes. The secondary effects should be stronger if holes (rather than trenches) are to be drilled in a bulk substrate.

3 3D photonic crystal fabrication

Photonic crystals are artificial structures created in high-refractive-index materials. A 3D photonic crystal has the potentiality of generating a full photonic band gap and thus controlling spontaneous light emissions in all space directions. Yablonovite [7], a mechanically realizable diamond-like structure, is proposed to fulfil the promise. However, such

a structure remains difficult to fabricate at small scale for wavelengths at (or below) the near-infrared range, essentially due to the short period (below 1 μm) that the short wavelength implies. Though various approaches have been proposed, the fabrication is limited to a small number of periods (≤ 3) in the third direction (thickness) [8–10].

The capacity of the FIB to etch extremely deep holes at submicrometer scale in a porous substrate provides a unique opportunity to fabricate Yablonovite in the near-infrared range. Yablonovite is a 3D lattice formed by three sets of holes along the (110), (101) and (011) directions of a face-centered-cubic (fcc) lattice [7], each set forming a 2D sublattice (see Fig. 3). The holes cross one another with their crisscrosses coinciding with the nodes of the same fcc lattice. The fabrication can thus be divided into two stages.

Firstly, a 2D triangular lattice, with a periodicity of 0.65 μm, is generated by photoelectrochemical etching in a low-doped monocrystalline silicon substrate. The holes (macropores) are about 50-μm deep [11]. This lattice has two functions: it forms the first sublattice along the (110) direction, and provides at the same time the porous structure for FIB etching (the photoelectrochemically etched holes also serve as pores). Secondly, the other two sets of holes, along the (101) and (011) directions (each forming an angle of 60 degrees with the first set), are generated by FIB etching, made possible thanks to the first set of holes, to achieve the full dimensionality.

In the second stage, the openings of the photoelectrochemically etched holes are used to guide the etching in order to allow the FIB positioning with sufficient precision. The points to etch are defined as the center of the openings, so that the first (110) plane in which the three sets of holes cross one another coincides with the substrate surface. The beam positioning is realized using the imaging mode of the same apparatus. The FIB parameters are the same as in Sect. 2. In order to drill larger holes the beam is scanned around its central position. Two etching sections A and B, containing the same number of hole openings, are defined on the substrate surface (see Fig. 4). The FIB enters the substrate in A and B by the hole openings and exits through the zone C on the sample side. The etching in each zone is performed in only one direction ((101) in A, (101) in B). A specially designed sample holder is used to ensure a precise orientation. The 3D structure thus obtained is inside the substrate, and can be milled out using the same FIB (see Fig. 4).

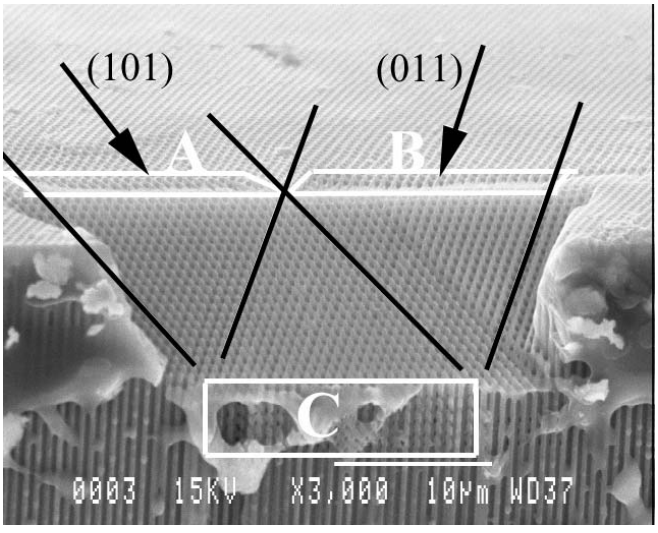

FIGURE 4 A sample after FIB etching and milling. The photoelectrochemically etched holes are perpendicular to the substrate surface (along the (110) direction). Their openings in the sections A and B are etched respectively along the (101) and (011) directions. The ion beam exits from the substrate side through the zone C

Photonic crystals up to 25 periods wide and five periods thick are fabricated using this method [12], which ensures an excellent geometrical precision. An area in the zone C is shown in Fig. 5. This sample is already milled out. The vertical holes are obtained by photoelectrochemical etching, the oblique ones by FIB etching. The precision of the FIB etching is high enough for the holes (one photoelectrochemically etched and two FIB-etched) to cross at the same point (see the amplified view in the same figure) after the FIB-etched ones have run through 25 μm inside the substrate. Reflection-spectra measurements are performed on these samples, where photonic band gaps are observed in the near-infrared range, in agreement with numerical simulations [13].

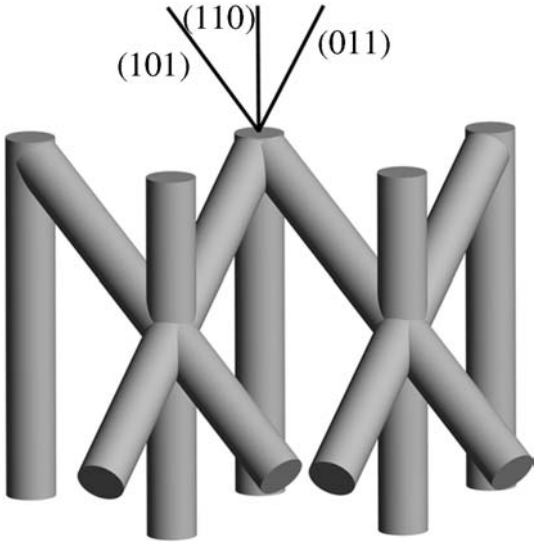

FIGURE 3 The three sets of holes that form the lattice of Yablonovite

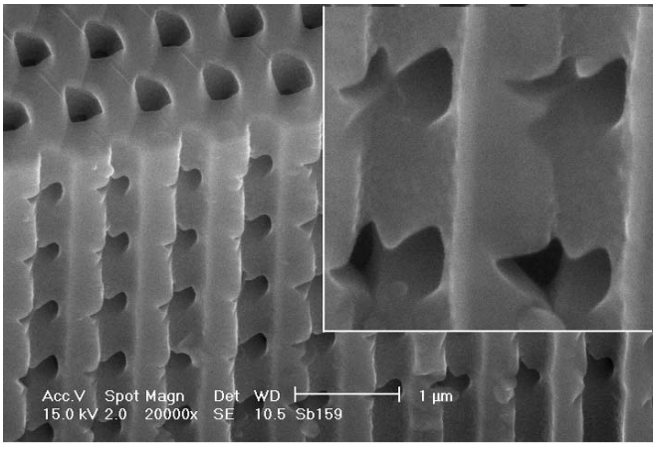

FIGURE 5 FIB-etched holes on the sample side where the beam exits. An amplified view is displayed on the *right*

4 Remarks

The above results demonstrate the capacity of the FIB etching to fabricate 3D lattices in a porous substrate. The combination of a FIB with chemical or plasma pre-etching opens new perspectives in the fabrication of various complex 3D objects at submicrometer or nanometer scale. The pre-etching allows the preliminary material removal and structuration indispensable for further FIB etching deep inside the substrate.

It is worth noting that, during FIB etching, though the total ion dose received for each pattern (especially deep ones) can be high, the total dose is distributed on the pore walls the beam traverses thanks to the porous structure, so that the effective dose for each wall is much weaker. As an example, for the deepest holes in the photonic crystals (35 periods), the total ion dose is estimated at about 1.8×10^{19} ions/cm^2, but the effective dose received by each wall is only about 5×10^{17} ions/cm^2. As pointed out, since the walls are etched in an almost independent way, the structural damage caused by ion irradiation is hoped to be weaker than in a bulk substrate for the same total ion dose.

It should also be pointed out that much of the sputtered material is redeposited into the pores inside the substrate. This will, or will not, strongly modify the porous structure, depending on the air-filling rate. If the latter is high enough, the porous structure will remain almost unchanged, as the walls are thin and the sputtered material will be of small quantity. The higher the air-filling rate, the less the redeposition. In the case of photonic crystal fabrication, the walls are about $0.1 \sim 0.2$ μm in thickness and the pores about $0.4 \sim 0.5$ μm in diameter; the material redeposition into the pores due to wall sputtering will not introduce a strong geometrical modification.

5 Conclusion

We have shown that the focused-ion beam has the capacity of etching extremely high-aspect-ratio patterns in a porous substrate. Three-dimensional lattices of submicrometer periodicity can thus be generated in combination with chemical pre-etching. Three-dimensional photonic crystal fabrication in the near-infrared range provides a demonstration.

REFERENCES

1 J. Melngailis: J. Vac. Sci. Technol. B **5**, 469 (1987)
2 H. Yamaguchi, A. Shimase, S. Haraichi, T. Miyauchi: J. Vac. Sci. Technol. B **3**, 71 (1985)
3 R.L. Kubena, R.L. Seliger, E.H. Stevens: Thin Solid Films **92**, 165 (1982)
4 Y. Ochiai, K. Shihoyama, T. Shiokawa, K. Toyoda, A. Masuyama, K. Gamo, S. Namba: J. Vac. Sci. Technol. B **4**, 333 (1986)
5 J.C. Beckman, T.H.P. Chang, A. Wagner, R.F.W. Pease: J. Vac. Sci. Technol. B **14**, 3991 (1996)
6 U. Gruning, V. Lehmann, S. Ottow, K. Bush: Appl. Phys. Lett. **68**, 747 (1996)
7 E. Yablonovitch, T.M. Gmitter, K.M. Leung: Phys. Rev. Lett. **67**, 2295 (1991)
8 S. Noda, N. Yamamoto, H. Kobayashi, M. Okano, K. Tomoda: Appl. Phys. Lett. **75**, 905 (1999)
9 J.G. Fleming, S.Y. Lin: Opt. Lett. **24**, 49 (1999)
10 C.C. Cheng, A. Scherer, R.T. Tyan, Y. Fainman, G. Withzgall, E. Yablonovitch: J. Vac. Sci. Technol. B **15**, 2764 (1997)
11 S. Rowson, A. Chelnokov, J.-M. Lourtioz: J. Lightwave Technol. **17**, 1989 (1999)
12 K. Wang, A. Chelnokov, S. Rowson, P. Garoche, J.-M. Lourtioz: J. Phys. D: Appl. Phys. **33**, L119 (2000)
13 A. Chelnokov, K. Wang, S. Rowson, P. Garoche, J.-M. Lourtioz: Appl. Phys. Lett. **77**, 2943 (2000)